Research on Engineering Structures & Materials
www.jresm.org

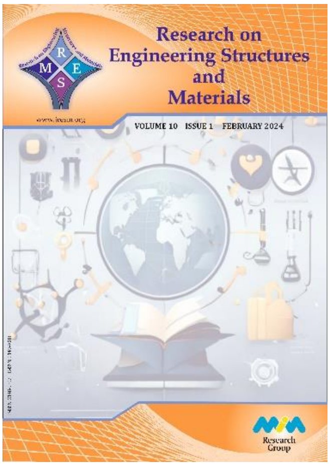

Results of Sn/Pb solder affected aluminum under wear study

Mohammad Salim Kaiser

Online Publication Date: 02 January 2024
URL: http://www.jresm.org/archive/resm2023.40me0818rs.html
DOI: http://dx.doi.org/10.17515/resm2023.40me0818rs
Journal Abbreviation: *Res. Eng. Struct. Mater.*

To cite this article
Kaiser MS. Results of Sn/Pb solder affected aluminum under wear study. *Res. Eng. Struct. Mater.*, 2024; 10(3): 957-972.

Research on Engineering Structures & Materials
www.jresm.org

Research Article

Results of Sn/Pb solder affected aluminum under wear study

Mohammad Salim Kaiser[a]

Innovation Centre, International University of Business Agriculture and Technology, Bangladesh

Article Info

Article history:

Received 29 Oct 2023
Accepted 02 Jan 2024

Keywords:

Al- alloy;
Corrosive;
Micrographs;
Sn- Pb solder;
Tribology;
Worn surfaces

Abstract

Nanostructured Al-Sn and Al-Pb alloys are effectively used to improve their wear characteristics. Taking this into consideration, the wear properties of aluminum have been studied while affected by both elements Sn-Pb solder at a lower level to explore its reusing potentials. In this purpose a common pin-on-disk device is used in which different dry, wet and corrosive sliding environments are applied. Additionally, pure Al, Al-Sn and Al-Pb alloys are also considered for recovering the clarification and to separate elemental effects on wear properties. The worn surfaces of the samples are examined using optical and scanning electron microscopy, both before and after wear. Surface roughness also is a measure to assess the wear properties under different environments. The findings revealed that minor solder has a great impact on the wear properties of Al with Sn playing a better role than Pb. Solid solution strengthening is the main reason for improved wear behavior in terms of the low wear rate and coefficient of friction. Both Sn and Pb do not form any intermetallic with Al but with impurities it can easily occur particularly with Sn resulting in better wear properties. This phenomenon is more prominent in corrosive environment than wet due to the protective oxide layer on the surfaces. In dry sliding conditions, numerous large wear particles, oxide debris and grooves can be seen on the worn surface, but smoother wear tracks are seen in wet and corrosive environments as form oxide film and thumbs down somewhat direct contact on the moveable surfaces. SEM analysis also reveals higher abrasive wear and plastic deformation on the worn surface produced under dry sliding conditions where minor added alloys indicating that reinforcing particles effectively influence the properties.

1. Introduction

From the beginning, aluminum has been one of the popular materials in many industries due to its excellent physical, mechanical, electrical, and chemical properties such as light density, high strength, wear, and corrosion resistance [1-3]. Its properties are enhanced many times when it is alloyed with other elements. Alloying has a limitation in that improving one property it may affect other properties. In the book by S. Sivashankaranto provides ample information about the effects of alloying elements on aluminum [4]. More precisely Si lowers the melting point, cumulative fluidity, and Cu provides precipitation hardening and strength, while reducing ductility as well as corrosion resistance. Mn enhances work hardening rate, but prevents cracking during stress corrosion., correspondingly Fe can enhance hardness and decrease tensile strength in addition to corrosion resistance. Ni addition improves strength at high temperature, at the expense of electrical conductivity. For grain refining as well as thermal stability minor Zr also added into the Al-alloys [5-7]. Sometimes aluminum alloys give better strength by heat treatment. Plastic deformation is another method of increasing the strength of aluminum and its alloys [4, 8, 9]. The favorable point of aluminum is that it can be recycled again and again

*Corresponding author: dkaiser.res@iubat.edu
[a]orcid.org/0000-0002-3796-2209
DOI: http://dx.doi.org/10.17515/resm2024.59ma1029rs

without losing its major character. The process involves just re-melting and it is much less expensive along with energy-intensive than making new aluminum from its original source. Recycling it also has significant environmental benefits by eliminating air and water pollution which need to process raw materials [10, 11]. Aluminum is extensively used in the manufacturing of electronic and microelectronic components, and in some countries for power lines. It is widely used in the manufacture of transformers, low-voltage rotors, motor capacitors and sometimes also used for antenna and radar construction [12]. Hence, Al-alloys are also claimed to be suitable for the aerospace industry [13, 14].

When used in this electrical sector, Al wires or parts are to be joined. Soldering is applied to the joining process. In this case the recycled aluminum content is a small amount of solder alloy [15, 16]. The best option is reusing the scraped materials at their leftover state for appropriate engineering applications. At earlier stages Sn-Pb solder alloys are mostly used. Therefore, cast aluminum will contain minor amounts of Sn and Pb. From this perspective, reused or melted scraped Al requires characterization of the properties achievable with special attention to surface behavior. Abrasion and friction properties of materials are the main component failures causing surface deformation and reduced durability [17, 18]. Some have reported the effect of Sn or Pb on the wear behavior of Al alloys where the levels of such elements were high [19, 20]. There is no work reported where Sn or Pb is used in small amounts as well as both elements simultaneously. Additionally, sufficient information on the tribological behavior of these alloys under water or saline environments is also lacking. Al-based bearings and associated fittings are preferred in corrosive environments, so it is necessary to have reliable data on friction and wear properties when alloys are applied to noncorrosive stainless steel counter bodies. Therefore, a significant effort has been taken to investigate these properties of Sn-Pb solder affected Al under different sliding conditions as mentioned above for applications in the marine sector.

2. Materials and Methods

The objective was to study the wear behavior of Sn-Pb solder affected Al under different conditions. Extensively old Al electrical wire and different soldered connecting electrical components were melted conventionally using a resistance heating furnace. From the chemical composition of melt aluminum, it contained the minor amount of 1.0~1.5wt% Sn and 1.0~1.5wt % Pb. To establish the influence separately of tin and lead in the Al, depending the minor elements another three more samples like pure Al, binary Al-Sn, Al-Pb were chosen. Commercially pure grade Al, Sn and Pb were taken for developing those alloys where mild steel mould of 155 x 45 x 35 mm size was used. The cast alloys were then subjected to homogenization and solutionizing at 450°C for 12 h and 530°C for 2 h respectively. The developed four samples consist the following elements analyzed by Optical Emission Spectroscopy as in Table 1. Additionally, Cu, Mg, Mn, Zn, Ni, Cr, Ti etc, were also present in the alloys as trace impurities.

Table 1. Alloys chemical composition by wt.%

Alloy	Sn	Pb	Fe	Si	Al
Pure Al	0.002	0.002	0.202	0.280	Bal
Al-Sn	1.512	0.012	0.314	0.335	Bal
Al-Pb	0.002	1.275	0.335	0.345	Bal
Al-Sn-Pb	1.433	1.201	0.406	0.435	Bal

For the physical, mechanical and wear test the cast and heat-treated alloy samples were machined to 145 x 40 x 32 mm size for skin out the oxide layer. Then the bar was cold rolled by 80% with a 10HP rolling mill where the 40 mm thick portion under gone to 8 mm. For wear study, size of 12 mm in length and 5 mm in diameter were machined from the cold rolled alloys. Alloy densities were calculated from the chemical composition. The alloys are aged at 100°C for one hour becoming the better strength [21]. The microhardness of the aged samples was measured using a Micro Vickers Hardness testing machine. One kg load and ten seconds dwell time were used there. Tensile testing was carried out according to ASTM E8 specification at room temperature in an Instron testing machine. The wear and frictional properties of tested alloys were investigated following ASTM standard G99-05 where a pin-on-disc type apparatus was used [22, 23]. As the counter surface material 309s stainless steel disc with 100 mm semi-dia and 15 mm thick was used. The hardness and roughness of the disc was around HRB 85 and was 0.39 μm respectively. The 20 N load, that is calculated contact pressure 1.02 MPa was used for wear study. Furthermore, 5 to 50 N loads were used for other experiments. During the wear study the disc was rotated at 200 rpm where the pin samples stay on a track diameter of 49 mm as a result the calculated sliding speed was 0.51 m/s. All the tests were completed in ambient conditions of 70% humidity and at 22 °C temperature. For an individual data five tests were carried out and the average of these values were considered. The specimens were first subjected to dry sliding conditions and then chronologically to the distilled water and then 3.5% NaCl saline water. For both the wet and corrosive environments, drip-type single-point at the contact interface of the sample and the steel counter plate was maintained with a constant rate of discharge throughout the experiment. The discharge rate was five drops per minute as controlled by the regulator. The specific wear rate was calculated from the measured weight loss (Δw), the running distance in the test (S.D.), and the normal load (L) applied to the samples [23]. The sliding distances were calculated from the track diameter and speed of rotation of the disc. The load cell reading (F) was normalized by the load applied, L to find out the friction coefficient (μ). The mathematical relations to obtain the weight loss, specific wear rate (S.W.R.) and the friction coefficient are stated by equations as follows:

$$\Delta W = W_{initial} - W_{final} \tag{1}$$

$$S.W.R. = \frac{\Delta W}{S.D. \times L} \tag{2}$$

$$\mu = \frac{F}{L} \tag{3}$$

The worn surface and wear debris of the specimens from the test were put under microstructural observation using USB digital microscope. In some cases, SEM analysis was used by JEOL scanning electron microscope.

3. Results and Discussion

3.1. Physical and Mechanical Properties

Table 2 displays the experimental results of physical and mechanical properties of commercially pure Al, binary Al-Sn, Al-Pb and solder affected ternary Al-Sn-Pb alloys including density, hardness, tensile strength and percent elongation. Pure Al exhibit lowest density, while Al-Sn shows higher for addition of 1.51 wt.% Sn. Similarly, 1.28wt% Pb is added to Al-Pb to continue the trend, and it is evident that the alloy with the highest density, Al-Sn-Pb, contains both added elements. The density of Al, Sn and Pb are 2.7gm/cm^3, 7.3gm/cm^3 and 11.34gm/cm^3 respectively. Hardness of the alloyed samples is higher due to the solid solution strengthening. Sn has the BCC crystal structure but Pb has the FCC structure as Al. As a result, Sn shows the higher hardness than Pb added alloy. Furthermore, both Sn and Pb elements do not form any intermetallic with Al but form intermetallic with trace impurities resulting in additional hardness with respect to Sn. Solder added alloys exhibit the result of two elements [24, 25].

The solder-affected Al shows the highest tensile strength in the aforementioned reason, followed by alloys containing Sn and Pb, and pure Al, which shows the lowest tensile strength. A small variation is observed in case of percentage of elongation. Maximum fraction of precipitates occurs into the solder affected alloy which hinders the dislocation movement so the lower elongation. For the same reason the result of elongation conforms the sequence of Al-Sn followed by Al-Pb and pure Al [26, 27].

Table 2. Physical and Mechanical properties of the experimental alloys

Alloy	Density, gm/cm^3	Hardness, VHN	UTS, MPa	% Elongation
Pure Al	2.709±0.008	51.4±1.5	114.4±4.5	10.7±1.1
Al-Sn	2.801±0.025	62.3±2.5	137.3±7.5	9.6±0.7
Al-Pb	2.826±0.025	52.8±2.3	123.8±6.5	10.2±0.7
Al-Sn-Pb	2.889±0.031	63.5±3.1	147.0±8.0	9.5±0.6

3.2. Wear Behavior

Figure 1 displays the average weight losses of pure Al, Al-Sn, and Al-Pb, as well as the weight loss of the Al-Sn-Pb alloy, with respect to sliding distance. The dry sliding conditions were maintained at a pressure of 1.02 MPa and a velocity of 0.51 m/s. As expected, weight loss was observed for all samples, but the degree of weight loss varied. As the sliding distance increased, the contact period between the rotating disk and the sample face also increased, leading to further weight loss. The variation in weight loss can be attributed to material properties such as hardness, density, and softening behavior, as shown in Table 2, while increases tensile strength, weight loss decreases [28, 29].

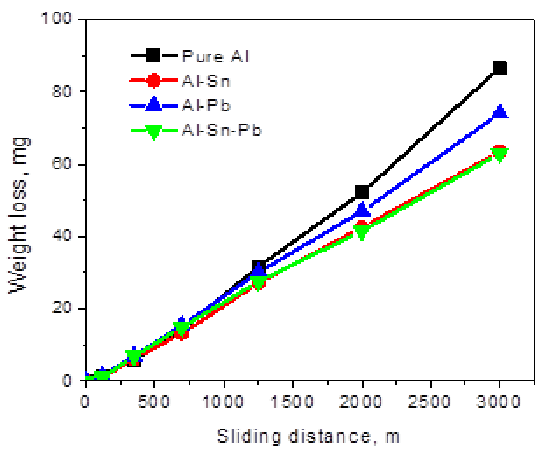

Fig. 1. Variation of the weight loss with sliding distance in dry sliding environment

Using Equations 1 and 2 calculated wear rates of investigated alloys mentioned above are plotted against the sliding distance. Whereas Fig. 2, 3 and 4 show the difference in wear rates in dry, wet and corrosive environments respectively. From the Fig. 2, it may be said that under dry sliding condition wear rate increase to certain distance followed by tends to a constant value. The increase in wear rate can be attributed to frictional heat by excessive pressure as prolonged intimate contact between the two mating surfaces and softening of materials [30]. So, it occurs more effectively. The highest wear rate is raised for pure Al trailed by Pb added alloy, Sn added alloy and finally the solder affected alloy. According to the Archard's theory wear rate in dry sliding condition of alloys is found to decrease with the increased hardness and found to be consistent with the result [31]. Besides, during wear tests, the generation of an intermediate oxide layer between mating surfaces is also one of the probable reasons for decreasing wear rate. Average values of two opposite effects are displayed in the graphs. For long time sliding contact the surfaces with air forms thick oxide layers which control the wear rate and favorable to the constant wear rate [23].

When sliding in distil water environment, the wear rate decreases some extend for all the alloys (Fig. 3). Throughout sliding the water by hydrogen attack form oxide which is relatively stable on the surface. Minor added alloys form higher oxides as protect the surface from wear. Once more, Sn oxide is more stable than that of Pb oxide as a result slightly the lower wear rate for Sn added as well as solder affected alloy [32]. More specifically in the case of ternary solder affected alloy the role of lower stable oxide of Pb dominates in high wear rates with sliding distance.

Except for pure Al more decreasing nature of wear rate is observed in case of corrosive 3.5% NaCl sliding environment. The wear rate radically reaches a constant value with the sliding distance (Fig. 4). In this case the corrosive wear serves as a clear indicator. Pure Al affected by corrosive attack, dissolute continuously or uniformly detached it wears out more quickly in the corrosive environment. In case of minor added alloys again, it is known that the foreign particles into the alloy is attacked more by the corrosion or oxidization. It may be noted that corrosive products are thought to be more stable on surfaces than when they form oxides in wet environment, resulting in lower wear rate [33]. The overall presence of wear rate variation with sliding distance in corrosive environments first increases then decreases and then increases again. The reason behind this increase in wear rate is due to the corrosive attack, next formation of passive films on the surface of the sample which acts as a barrier against further corrosion hence the wear rate is low. After some time, the wear rate increases due to the gradual breakdown of the progressively thicker passive films [34].

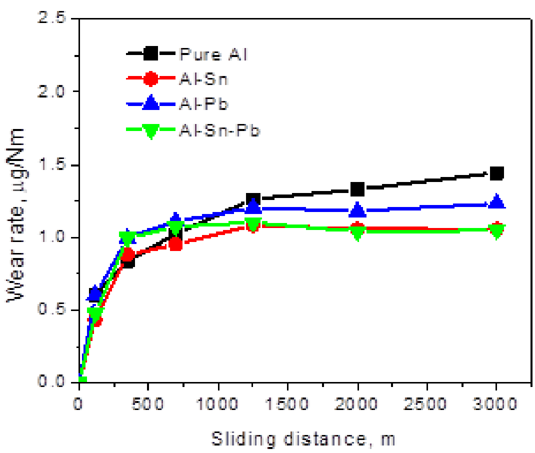

Fig. 2. Variation of wear rate with sliding distance in dry sliding environment

The results of the friction coefficient with different sliding distances are shown in Figures 5-7 for four specimens under dry, wet and corrosive tested environment, respectively. In all cases the friction coefficient is initially low and then rises with increasing sliding distance. The friction coefficient values are initially low due to the contact between the rough layers on the specimen and the disc material. Within a short sliding distance, the friction coefficient increases. This is because the cracking and removal of the surface oxide layer leading to metal-to-metal contact increases the coefficient of friction. With increasing sliding distance, interface temperatures can develop which can promote surface oxidation thereby reducing the direct contact of the surfaces hence slightly reducing the friction coefficient [35].

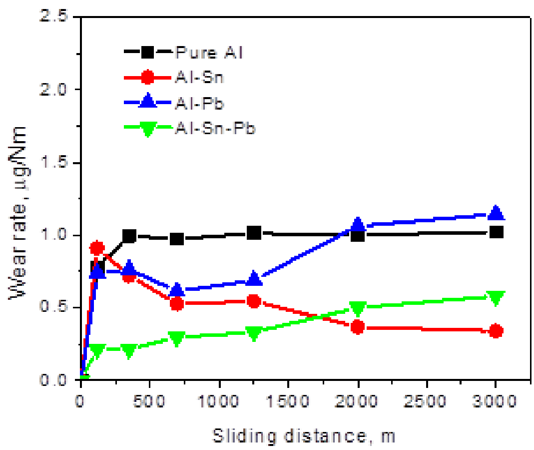

Fig. 3. Variation of wear rate with sliding distance in wet sliding environment

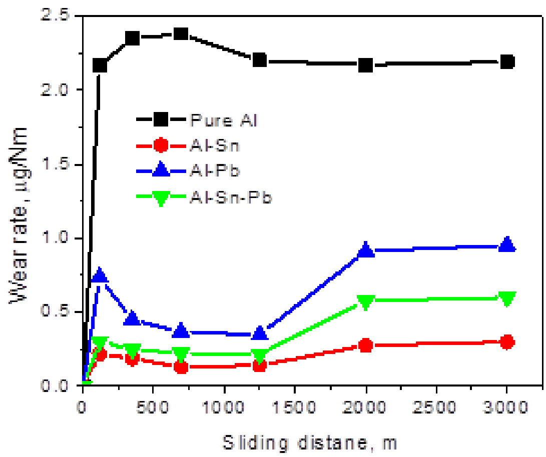

Fig. 4. Variation of wear rate with sliding distance in corrosive sliding environment

The coefficient of friction for all the alloys in the dry environment is much greater than under wet and corrosive environment. The cause of this friction reduction is the “Sealing Effect”, which reduces the roughness of the surfaces in contact [36, 37]. In all the cases the coefficient of friction of commercially pure aluminum shows the highest and solder affected Al-Sn-Pb alloy the lowest followed by tin added Al-Sn and then lead added Al-Pb alloy and the result is in good agreement with the observed microhardness value of the alloys. Differences in the extent of localized plastic deformation at real contact areas may lead to the deficiencies in friction coefficient. The solder affected alloy exhibits the lowest friction as it is the hardest one and undergo lowest plastic deformation [38]. Furthermore, solid solubilities of Sn and Pb in Al are less than 0.02 and 0.026 wt% at room temperature, therefore, the soft Sn and Pb phase can form compact structure particles in the Al-matrix and act as solid lubricants. Some deviation is observed under water and saline environment as controlled by the oxidization and corrosion created by the minor added elements on the surfaces [24, 39]. The initial friction coefficient for all alloys is high due to the high roughness created by the dense saline particles as well as the rough matting surface. After some time, the corrosive product fills the voids and acts as a sealing effect.

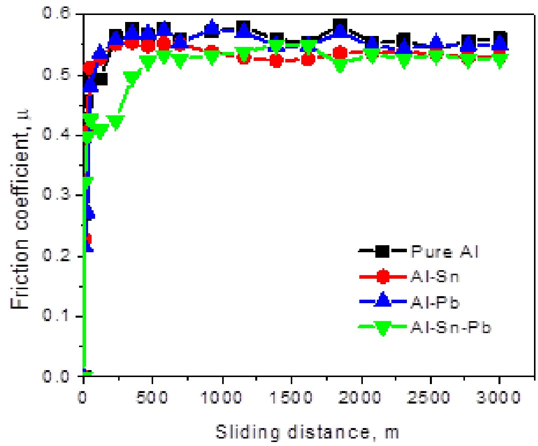

Fig. 5. Variation of the coefficient of friction with sliding distance in dry sliding environment

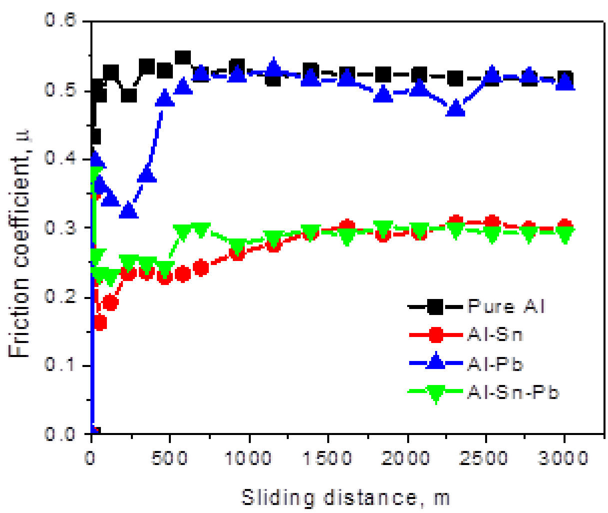

Fig. 6. Variation of the coefficient of friction with sliding distance in wet sliding environment

The nature of friction under different loads and environments at a constant velocity of 0.51 m/s is presented in Figures 8, 9 and 10. The friction coefficient in dry sliding condition shows a normal nature of decreasing trend as it may be related to the development of oxide layers (Fig. 8). But beyond a certain load the coefficient increases and pure Al exhibits the lowest coefficient and solder affected Al shows the highest followed by alloys containing Sn and Pb. Alloys soften due to stress and temperature effects under high level loads whereas alloys with first Sn and then Pb binary inclusions reflect higher coefficients for their lower melting temperatures. Both alloy effects show the highest intensity with the solder affected alloy.

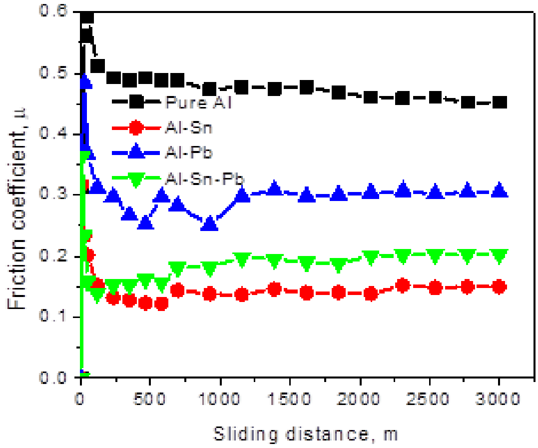

Fig. 7. Variation of the coefficient of friction with sliding distance in corrosive sliding environment

However, under wet sliding condition all the samples show the decreasing trends of coefficient of friction with the applied loads (Fig. 9). In this case higher loads produces some oxide layer due to presence of water but it inhibits the heat generation as a result lower friction. The oxide layer formation of the individual alloys along with sealing effects reduces these coefficients.

Additionally, under corrosive condition, the level of friction coefficient fully controlled by the saline water (Fig. 10). Stable oxide layer forms by the Sn is higher than that of Pb as a result lower friction and both elements effects with higher oxide formation is reflected on the solder added alloy. The sealing effect also more active with high dense of this thin lubricating film of water on the surfaces [40, 41].

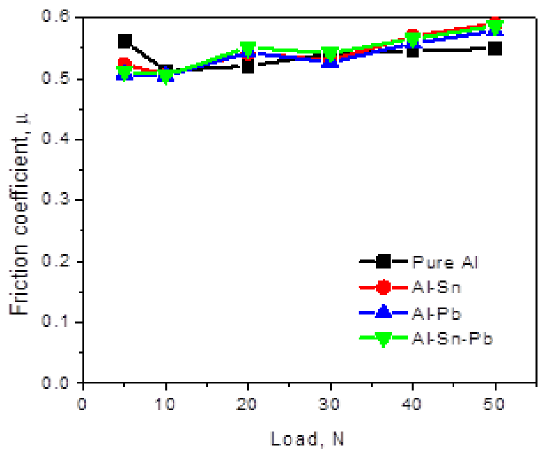

Fig. 8. Nature of friction coefficient in the dry sliding environment with loads

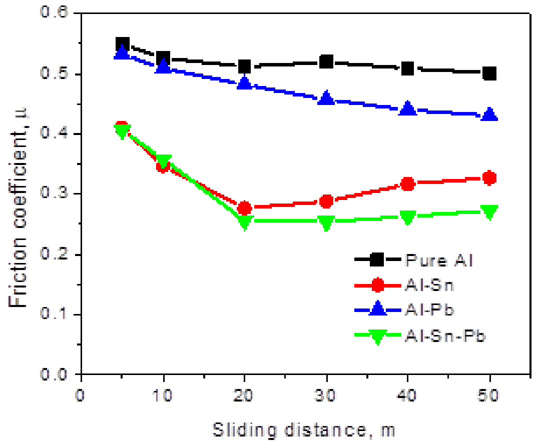

Fig. 9. Nature of friction coefficient in the wet sliding environment with loads

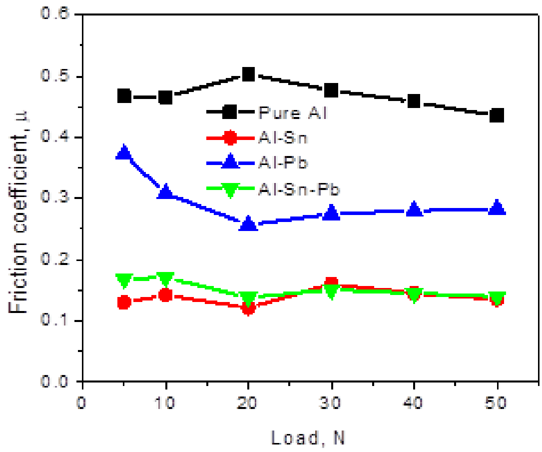

Fig. 10. Nature of friction coefficient in the corrosive sliding environment with loads

3.3 Optical Microscopy

Optical images of worn surfaces of pure Al, Al-Sn and Al-Pb and solder affected Al-Sn-Pb alloys before and after wear under dry, wet and corrosive sliding environments are presented in Figure 11. A pressure of 1.02 MPa applied throughout, a sliding velocity of 0.51m/s and a sliding distance of 3000m were used. The worn surfaces before wear demonstrate some scatter mark throughout the direction to polish as created by the metallographic polishing paper. Additionally, the surfaces display some different tones since various levels of alloying elements are present in alloys. Normally, this type of alloy consists of α-Al phase along with the second phases depending on the element present into the materials. Trace impurities also form intermetallic into in the interdendritic region. Without etching, the polished microstructure does provide the enough information without some color changes depending on the elements present [42].

When the alloys are tested under dry sliding conditions numerous large wear particles, oxide debris and the furrows are shown in the figure. Furthermore, the plastic deformation and numerous significant cracks can be seen. A significant amount of material is seen to be delaminating. It can also be observed from the figure, polish marks in the worn surfaces are fully absent on the surfaces as the delamination are occurred through removing the particles. The worn surface of solder affected along with minor added alloys show the surface morphology of low cracks but higher oxide layer indicating the white color on the surface compare to base metal pure Al. The wear scars and fragments show how abrasive wear, delamination wear, and oxidation wear all contribute to wear [43].

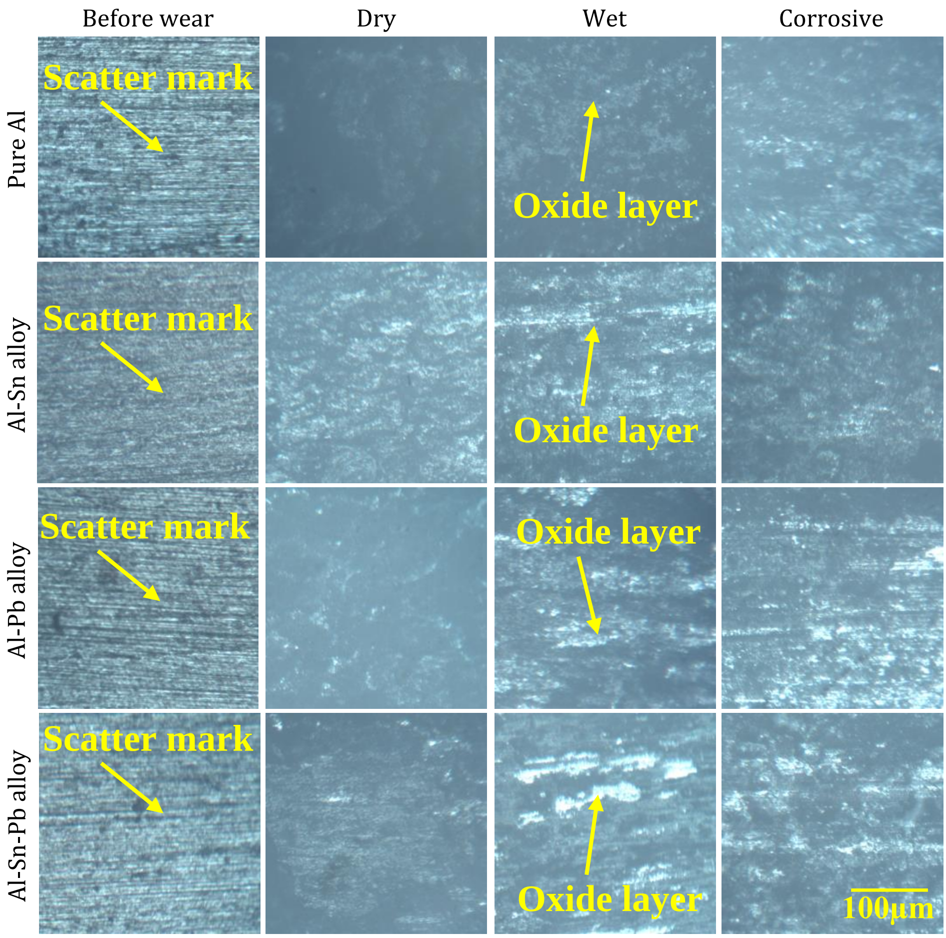

Fig. 11. Optical micrograph of polished surfaces of experimental alloys before and later wear in the condition of dry, wet and corrosive sliding for 3000m at applied pressure of 1.02 MPa

In contrast, the wear tracks visible on the worn surface are smoother in a wet environment. Hardly any cracks are visible. In addition, the debris and grooves are only visible in a few places. Additionally, due to the lubricating and cooling effects, some dark areas can be seen. The liquid environment reduced the heat concentration, local stress, and friction of shear, which prevented the formation of cracks and debris. Furthermore, during the sliding process, the majority of particles and debris are washed away by water, minimizing abrasive wear. As a result, the liquid environment's frictional characteristics are much better than those of the surrounding air. However, in the 3.5% NaCl corrosive environment, the wear mechanism is altered. Actually, the corrosion-wear that occurred in the corrosive fluid is what produced the oxidation film. During the wear testing, the oxides are subsequently broken down, and wear debris is produced. Additionally, heat from the friction is produced at the interface, which prompt the growth of more oxides. Change of surfaces color also confirm it. The size of the debris and particles is smaller than that of the dry sliding condition, and there are no signs of a crack or plastic deformation [43].

Figure 12 shows the dust particles that were created during the wear test of four experimental alloys when they were sliding in a dry environment. Granular alloy dust is present, and some of the chips are composed of stainless-steel discs. For each alloy, the quantity of steel chips in the dust varies. Pure Al dust has very little chips because of its low hardness. Sn-containing alloy dust has more chips than Pb-containing alloy dust, which results in a higher hardness. For maximum hardness, the majority of chips are produced in solder-affected alloy [44].

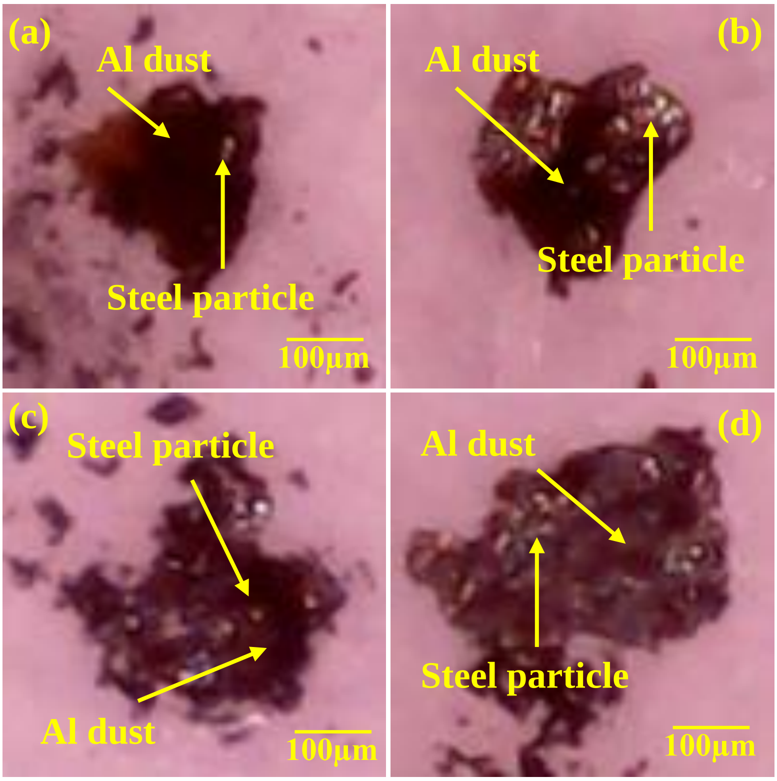

Fig. 12. Optical micrograph of generated dust from the different samples wear under dry sliding condition (a) pure Al (b) Al-Sn, (c) Al-Pb and (d) Al-Sn-Pb alloys

3.4. Scanning Electron Microscopy

Again, an attempt has been made for better understanding, SEM microphotographs of the worn surfaces of four samples after dry sliding wear at a distance of 3000 m are presented in Fig. 13. All the pure Al along with other binary Al-Sn, Al-Pb and ternary solder affected Al-Sn-Pb alloys clearly suggesting abrasive wear. The worn surfaces after the wear tests of pure Al showed a two-body abrasive wear with predominance of plow groove regions, indicating abrasive wear by plastic deformation, and some regions with adhesive wear, featured by a rough aspect due to the occurrence of delamination (Fig. 13a). In case of Sn and Pb added alloy, the corresponding phases are present in respected worn surfaces (Fig.

13b and 13c). The solder affected alloy obviously indicates both the phases which dominate the wear properties (Fig. 13d) [45].

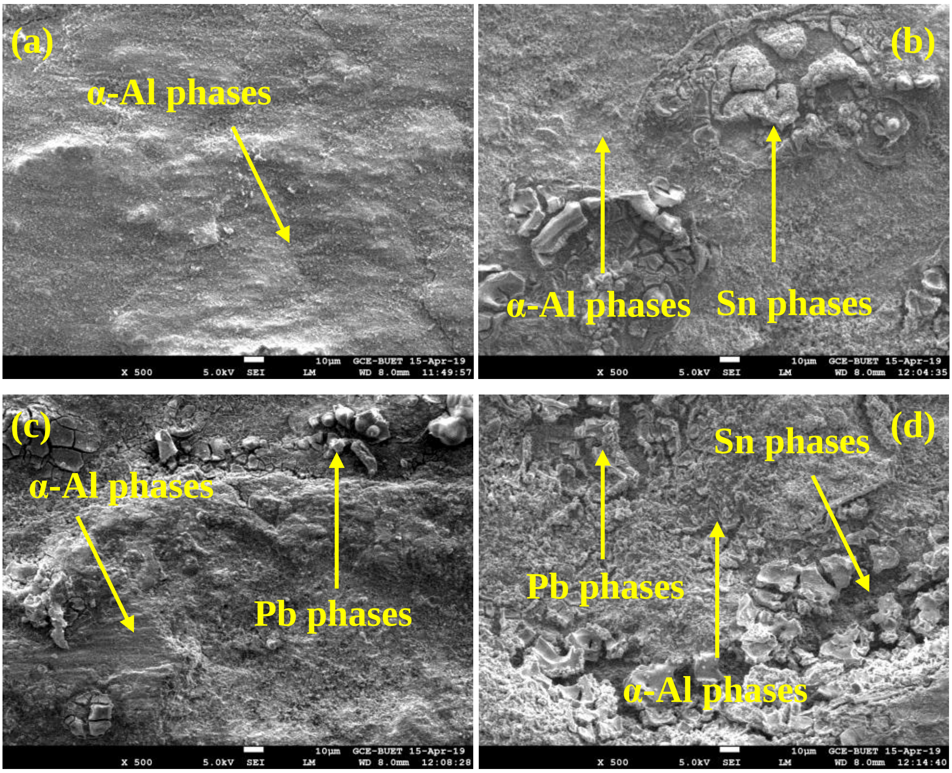

Fig. 13. SEM images of worn surfaces after dry sliding wear under 1.02 MPa pressure for a distance of 3000 m, a) pure Al, b) Al-Sn, c) Al-Pb and d) solder affected Al-Sn-Pb alloys

3.5. Roughness

Dry, wet and corrosive environments are used to compare the roughness levels of all four alloys. Figure 14 displays a bar graph of the results. In the dry sliding condition, pure Al exhibits the highest relative roughness, while Pb and Sn add-on alloy resemble those with solder. It is evident that the surface's softness causes more wear marks. This is connected to this phenomenon. Table 2 has been made available to demonstrate the hardness and other properties of materials. When exposed to water in wet environments, the alloy's roughness decreases due to a reduction in direct contracting between matting surfaces. Consequently, there are not enough differences between alloys. In contrast, corrosive wear can result in the presence of NaCl corrosion product on surfaces. Under pressure and temperature, the surface becomes smooth. Consequently, the roughness in this corrosive environment is inferior and entirely depends on the occurrence of rust [34, 46].

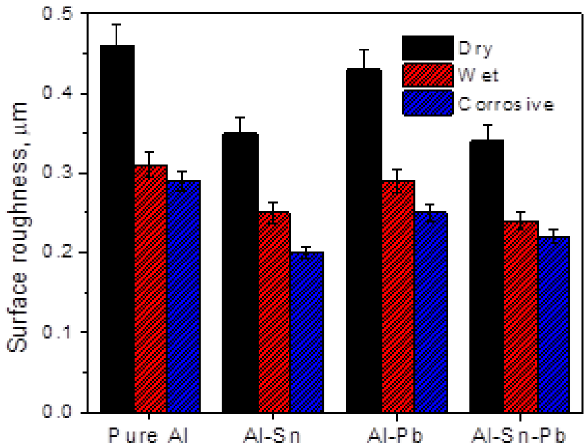

Fig. 14. Surface roughness of the samples worn surfaces under different sliding conditions

4. Conclusions

This study investigated the wear characteristics of commercially pure aluminum affected by Sn-Pb solder and compares the influence of wet and corrosive with the dry sliding condition and the conclusions can be drawn from the study as follows.

- When affected by Sn/Pb solder the tribological characteristics of commercially pure Al improves in terms of low specific wear rate and friction coefficient. Where tin plays a better role compare to lead. Solid solution strengthening is the key reason for better wear performance. Both Sn and Pb do not form any intermetallic with Al but with impurities it can easily ensnare for Sn resulting in better wear properties.
- The highest wear rate is observed under dry sliding conditions due to thermal softening of the material but under distilled water sliding condition wear rate decreases as it holds back the heat generation to prevent the softening of contact materials. The decreasing nature continued in 3.5% NaCl saline water environment due to the formation of stable oxide layer on the surfaces along with the reduced direct contact.
- The friction coefficient is solder affected alloy is the lowest than Al followed by Sn added and Pb added alloy due to better strength, as the low plastic deformation of the material at real contact areas may lead to the lack of friction coefficient. However, in a wet sliding environment every coefficient of friction decreases due to the sealing effects and corrosive environment in addition to the corrosive oxide layer as controlled the friction.
- Optical microscopy confirms the visible wear tracks on worn surfaces are smoother in a wet and corrosive environment than in a dry sliding environment due to avoid softening and preventing direct contact between the two mating surfaces.
- SEM analysis indicates higher abrasive wear and plastic deformation on the worn surfaces wear under dry sliding condition. Whereas minor added alloys show Sn and Pb phase particles in this matrix then perform by way of solid lubricants.
- The solder affected alloy exhibits the lowest relative roughness followed by Sn, Pb and Al due to less wear marks resulting in higher surface hardness. In a wet sliding environment, alloys roughness is reduced due to reduced direct contact between

the matting surfaces. Under saline environment smooth corrosive products fill-up, the gap between wear mark on the surface which further reduces the roughness.

Acknowledgement

It is acknowledged that the Miyan Research Institute of International University of Business Agriculture and Technology, Dhaka, provided financial support for the project work. The author would like to express his appreciation to Prof. Selina Nargis, the Director of Administration, for all of the helpful support and encouragement she has made available in advancing research activities at the university.

References

[1] ASM Handbook Committee. Properties and Selection: Nonferrous Alloys and Special-Purpose Materials. ASM International; 1990.
[2] Wang F, Li Y, Chen X, Zhao H, Yaqoob K, Du Y, Wang Z, Song M. Superior strength-ductility combination in Al alloys via dislocation gradient structure. Materials Research Letters. 2023;11(5):347-353. https://doi.org/10.1080/21663831.2022.2151851
[3] Ashkenazi D. How aluminum changed the world: A metallurgical revolution through technological and cultural perspectives. Technological Forecasting and Social Change. 2019;143:101-113. https://doi.org/10.1016/j.techfore.2019.03.011
[4] Sivasankaran S. Aluminium Alloys - Recent Trends in Processing, Characterization, Mechanical Behavior and Applications. IntechOpen; 2017. https://doi.org/10.5772/68032
[5] Kaiser MS, Sabbir SH, Kabir MS, Soummo MR, Nur MA. Study of mechanical and wear behaviour of hyper-eutectic Al-Si automotive alloy through Fe, Ni and Cr addition. Materials Research. 2018;2(4):1-9. https://doi.org/10.1590/1980-5373-mr-2017-1096
[6] Kaypour H, Gholamipour R, Khodabandeh A, Sabet H, Tayebi M. Work Hardening and Kinetics Analysis of Al0.3MnCrCoFeNi High-Entropy Alloy. The Journal of The Minerals, Metals & Materials Society (TMS). 2023;75:4171-4181. https://doi.org/10.1007/s11837-023-06040-w
[7] Kaiser MS. Solution treatment effect on tensile, impact and fracture behaviour of trace Zr added Al-12Si-1Mg-1Cu piston alloy. Journal of The Institution of Engineers (India): Series D. 2018;99(1):109-114. https://doi.org/10.1007/s40033-017-0140-5
[8] Ng CH, Yahaya SNM, Majid AAA. Reviews on aluminum alloy series and its applications. Academia Journal of Scientific Research. 2017;5(12):708-716.
[9] Kaiser MS, Datta S, Roychowdhury A, Banerjee MK. Age Hardening Behavior of Wrought Al-Mg-Sc Alloy. Materials and Manufacturing Processes. 2007;23(1):74-81. https://doi.org/10.1080/10426910701524600
[10] Paraskevas D, Ingarao G, Deng Y, Duflou JR, Pontikes Y, Blanpain B. Evaluating the material resource efficiency of secondary aluminium production: A Monte Carlo-based decision-support tool. Journal of Cleaner Production. 2019;215:488-496. https://doi.org/10.1016/j.jclepro.2019.01.097
[11] Luo AA. Recent advances in light metals and manufacturing for automotive applications. CIM Journal. 2021;12(3):79-87. https://doi.org/10.1080/19236026.2021.1947088
[12] Davis JR. Alloying: Understanding the Basics. ASM International; 2001. https://doi.org/10.31399/asm.tb.aub.9781627082976
[13] Saraçyakupoğlu T. Failure analysis of J85-CAN-15 turbojet engine compressor disc. Engineering Failure Analysis. 2021;119(104975). https://doi.org/10.1016/j.engfailanal.2020.104975

[14] Saraçyakupoğlu T. Fracture and failure analysis of the trainer aircraft rudder pedal hanger. Engineering Failure Analysis. 2021;122(105254). https://doi.org/10.1016/j.engfailanal.2021.105254
[15] Guan Q, Hang C, Li S, Yu D, Ding Y, Wang X, Tian Y. Research progress on the solder joint reliability of electronics using in deep space exploration. Chinese Journal of Mechanical Engineering. 2023;36(22):1-13. https://doi.org/10.1186/s10033-023-00834-4
[16] Kaiser MS. Effect of trace impurities on the thermoelectric properties of commercially pure aluminium. Materials Physics and Mechanics. 2021;47(4):582-591.
[17] Davim JP. Tribology for Engineers: A Practical Guide. Elsevier Science; 2011. https://doi.org/10.1533/9780857091444
[18] Katiyar JK, Ruggiero A, Rao TVVLN, Davim JP. Industrial Tribology. CRC Press, Taylor & Francis; 2022. https://doi.org/10.1201/9781003243205
[19] Zhu M, Gao Y, Chung CY, Che ZX, Luo KC, Li BL. Improvement of the wear behaviour of Al-Pb alloys by mechanical alloying. Wear. 2000;242(1-2):47-53. https://doi.org/10.1016/S0043-1648(00)00397-5
[20] Liu X, Zeng MQ, Ma Y, Zhu M. Wear behavior of Al-Sn alloys with different distribution of Sn dispersoids manipulated by mechanical alloying and sintering. Wear. 2008;265(11-12):1857-1863. https://doi.org/10.1016/j.wear.2008.04.050
[21] Kaiser MS. Trace impurity effect on the precipitation behaviour of commercially pure aluminium through repeated melting. European Journal of Materials Science and Engineering. 2020;5(1):37-48. https://doi.org/10.36868/ejmse.2020.05.01.037
[22] ASTM G99-05, Standard Test Method for Wear Testing with a Pin-on-Disk Apparatus. American Society for Testing and Materials; 2010.
[23] Khan AA, Kaiser MS. Wear Studies on Al-Si Automotive Alloy under Dry, Fresh and Used Engine Oil Sliding Environment. Research on Engineering Structures and Materials. 2023;9(1):1-18. https://doi.org/10.17515/resm2022.505ma0816
[24] McAlister AJ. The Al-Pb (Aluminum-Lead) system. Bulletin of Alloy Phase Diagrams. 1984;5:69-73. https://doi.org/10.1007/BF02868728
[25] McAlister AJ, Kahan DJ. The Al-Sn (Aluminum-Tin) System. Bulletin of Alloy Phase Diagrams. 1983;4:410-414. https://doi.org/10.1007/BF02868095
[26] Xu P, Luo H, Li S, Lv Y, Tang J, Ma Y. Enhancing the ductility in the age-hardened aluminum alloy using a gradient nanostructured structure. Materials Science and Engineering: A. 2017;682:704-713. https://doi.org/10.1016/j.msea.2016.11.090
[27] Ard PM, Uthaisangsuk V, Tosangthum N, Sheppard P, Wila P, Tongsri R. Fe-Sn Intermetallics Synthesized via Mechanical Alloying-Sintering and Mechanical Alloying-Thermal Spraying. In Key Engineering Materials. 2015;659:329-334. https://doi.org/10.4028/www.scientific.net/KEM.659.329
[28] Kaiser S, Kaiser MS. Comparison of wood and knot on wear behaviour of pine timber. Research on Engineering Structures and Materials. 2020;6(1):35-44. https://doi.org/10.17515/resm2019.115ma0207
[29] Baser E, Incesu A, Sismanoglu S, Gungor A. Wear performance investigation of AlSi8Cu3Fe aluminum alloy related to aging parameters. Research on Engineering Structures and Materials. 2019;5(2):99-105. https://doi.org/10.17515/resm2018.64is0829
[30] Prabhudev MS, Auradi V, Venkateswarlu K, Siddalingswamy NH, Kori SA. Influence of Cu Addition on Dry Sliding Wear Behaviour of A356 Alloy. Procedia Engineering. 2014;97:1361-1367. https://doi.org/10.1016/j.proeng.2014.12.417
[31] Archard JF. Contact and rubbing of flat surfaces. Journal of Applied Physics. 1953;24:981-988. https://doi.org/10.1063/1.1721448
[32] Duan XY, Li JR, Chang LM, Yang CW. A comparison of electrochemical oxidation performance of PbO2 and SnO2 electrodes. Journal of Water Reuse and Desalination. 2016;6(3):392-398. https://doi.org/10.2166/wrd.2016.150

[33] Farooq SA, Raina A, Haq MIU, Anand A. Corrosion Behaviour of Engineering Materials: A Review of Mitigation Methodologies for Different Environments. Journal of The Institution of Engineers (India): Series D. 2022;103:639-661. https://doi.org/10.1007/s40033-022-00367-5

[34] Kaiser MS, Sabbirb SH, Rahman M, Kabir MS, Nur MA. Effect of Fe, Ni, and Cr on the Corrosion Behaviour of Hyper-eutectic Al-Si Automotive Alloy in 3.5% NaCl Solution at Different Temperature and Velocity. Journal of Mechanical Engineering, The Institution of Engineers, Bangladesh. 2018;48(1):11-17. https://doi.org/10.3329/jme.v48i1.41083

[35] S. Dhanasekaran and R. Gnanamoorthy. Dry sliding friction and wear characteristics of Fe-C-Cu alloy containing molybdenum di sulphide. Materials and Design. 2007;28(4):1135-1141. https://doi.org/10.1016/j.matdes.2006.01.030

[36] Meyer WE., Walter JD. Frictional Interaction of Tire and Pavement, STP 793. American Society for Testing and Materials, USA.1983. https://doi.org/10.1520/STP793-EB

[37] Davim JP. Progress in Green Tribology: Green and Conventional Techniques. De Gruyter; 2017. https://doi.org/10.1515/9783110367058

[38] Moore, A. J. W., & Tegart, W. J. M. (1952). Relation between friction and hardness, Proceedings of the Royal Society of London. Series A. Mathematical and Physical Sciences, 212(1111), 452-458. https://doi.org/10.1098/rspa.1952.0234

[39] X. Liu, M.Q. Zeng, Y. Ma, M. Zhu. Wear behavior of Al-Sn alloys with different distribution of Sn dispersoids manipulated by mechanical alloying and sintering, Wear, Volume 265, Issues 11-12, 2008, Pages 1857-1863. https://doi.org/10.1016/j.wear.2008.04.050

[40] R. Tyagi, D. S. Xiong, J. Li and J. Dai. "Effect of load and sliding speed on friction and wear behavior of silver/h-BN containing Ni-base P/M composites. Wear, vol. 270, no. 7-8, pp. 423-430, 2011. https://doi.org/10.1016/j.wear.2010.08.013

[41] Zmitrowicz A. Wear debris: A Review of properties and constitutive models. Journal of Theoretical and Applied Mechanics. 2005;43(1):3-35.

[42] Kaiser MS, Qadir MR, Dutta S. Electrochemical corrosion performance of commercially used aluminum engine block and piston in 0.1M NaCl. Journal of Mechanical Engineering. 2015;45(1):48-52. https://doi.org/10.3329/jme.v45i1.24384

[43] Kaiser MS, Matin MA, Shorowordi KM. Role of magnesium and minor zirconium on the wear behavior of 5xxx series aluminum alloys under different environments, Journal of Mechanical and Energy Engineering. 2020;4(3):209-220. https://doi.org/10.30464/jmee.2020.4.3.209

[44] Rahman MM, Ahmed SR. Dry Sliding Friction and Wear of SnPb-Solder Affected Copper against Stainless Steel Counter Surface. Iranian Journal of Materials Science and Engineering. 2021;18(4):1-12.

[45] Billur CA, Gerçekcioglu E, Bozoklu M, Saatçi B, Ari M, Nair F. The electrical, thermal conductivity, microstructure and mechanical properties of Al-Sn-Pb ternary alloys. Solid State Sciences. 2015;46:107-115. https://doi.org/10.1016/j.solidstatesciences.2015.06.005

[46] Davim JP. Wear of Advanced Materials. John Wiley & Sons; 2013. https://doi.org/10.1002/9781118562093